



INSTITUT DE FRANCE
Académie des sciences

Comptes Rendus

Chimie

Mariana Zavagna-Witt, Nazir Tahir, Vasilica Alisa Arus, René Roy
and Abdelkrim Azzouz

**Synthesis of exopolysaccharide-based organo-montmorillonite with
improved affinity towards carbon dioxide and hydrophilic character**


Volume 25, Special Issue S3 (2022), p. 217-225

Published online: 3 May 2022

<https://doi.org/10.5802/crchim.175>

Part of Special Issue: Active site engineering in nanostructured materials for
energy, health and environment

Guest editors: Ioana Fechete (Université de Technologie de Troyes, France)
and Doina Lutic (Al. I. Cuza University of Iasi, Romania)

 This article is licensed under the
CREATIVE COMMONS ATTRIBUTION 4.0 INTERNATIONAL LICENSE.
<http://creativecommons.org/licenses/by/4.0/>



*Les Comptes Rendus. Chimie sont membres du
Centre Mersenne pour l'édition scientifique ouverte*
www.centre-mersenne.org
e-ISSN : 1878-1543



Active site engineering in nanostructured materials for energy, health and environment /
Ingénierie de sites actifs dans les matériaux nanostructurés pour l'énergie, la santé et l'environnement

Synthesis of exopolysaccharide-based organo-montmorillonite with improved affinity towards carbon dioxide and hydrophilic character

Mariana Zavagna-Witt^a, Nazir Tahir^b, Vasilica Alisa Arus^c, René Roy^a
and Abdelkrim Azzouz^{*, a, d}

^a Département de Chimie, Université du Québec à Montréal, Montreal, QC H3C3P8, Canada

^b Department of Chemistry and Biochemistry, University of Windsor, Windsor, ON N9B3P4, Canada

^c Catalysis and Microporous Materials Laboratory, Vasile Alecsandri University of Bacau, Bacau 600115, Romania

^d École de Technologie Supérieure, Montréal, QC H3C1K3, Canada

E-mails: marianazw@yahoo.com.br (M. Zavagna-Witt), nazir.tahir@uwindsor.ca (N. Tahir), arusalisa@yahoo.com (V. A. Arus), roy.rene@uqam.ca (R. Roy), azzouz.a@uqam.ca (A. Azzouz)

Abstract. Grafting of a bio-sourced exopolysaccharide (EPS) using a disulfide ethyl moiety with two ammonium ends as interface on Na⁺-exchanged montmorillonite (NaMt) turned out to be a “green” route to produce an OH-enriched organoclay with improved affinity towards CO₂ and moisture. Characterization through X-ray diffraction, infrared spectroscopy and thermogravimetric analysis revealed an organized structure with an increased basal spacing that facilitates the diffusion of CO₂ and water molecules and thermal stability up to 190 °C. Measurements through thermal programmed desorption (TPD) showed that at least 16 CO₂ molecules are adsorbed per OH group incorporated via HO:CO₂ interactions between CO₂ molecules and both EPS, and adsorbed water molecules. Adsorbed CO₂ can be completely released below 190 °C. This opens promising prospects for designing respiratory devices that support vegetal-derived moieties that can capture non-stoichiometric amounts of CO₂ in CO₂-rich gas mixtures and enclosures with non-thermal regeneration.

Keywords. Montmorillonite, Exopolysaccharide, Chemical grafting, CO₂ capture, Surface basicity, Thermal programmed desorption.

Published online: 3 May 2022

* Corresponding author.

1. Introduction

The contribution of carbon dioxide (CO₂) to global warming [1,2] has focused more interest on gas capture methods from flue emissions such as Temperature Swing Adsorption (TSA) and Pressure Swing Adsorption (PSA) [3–5] than on the reduction of CO₂ emissions at their very sources. Among the wide variety of adsorbents tested so far [6,7], amines, supported amines and base-like materials have alarmingly been believed as promising CO₂ adsorbents notwithstanding that they unavoidably generate undesirable carbamates and carbonates that need to be removed or thermally regenerated due to strong adsorbent-CO₂ chemical interaction [8].

Other CO₂ capture attempts were performed with materials such metal–inorganic–organic core–shell material [9], chemically modified activated carbon with nitric acid and ammonium aqueous solutions [10], cupric nitrate [11] or polyacrylonitrile [12], functionalized carbonaceous and silica-based materials [13], zeolites and layered double hydroxides [14–16], metal–organic frameworks (MOFs), mesoporous silica, clay, porous carbons, porous organic polymers (POP), and metal oxides (MO) [16]. Most of these materials involve costly/sophisticated synthesis procedures but low surface affinity as reported to their specific surface area as defined earlier [17]. They often act via a combination of physical–chemical interactions without a truly reversible of CO₂.

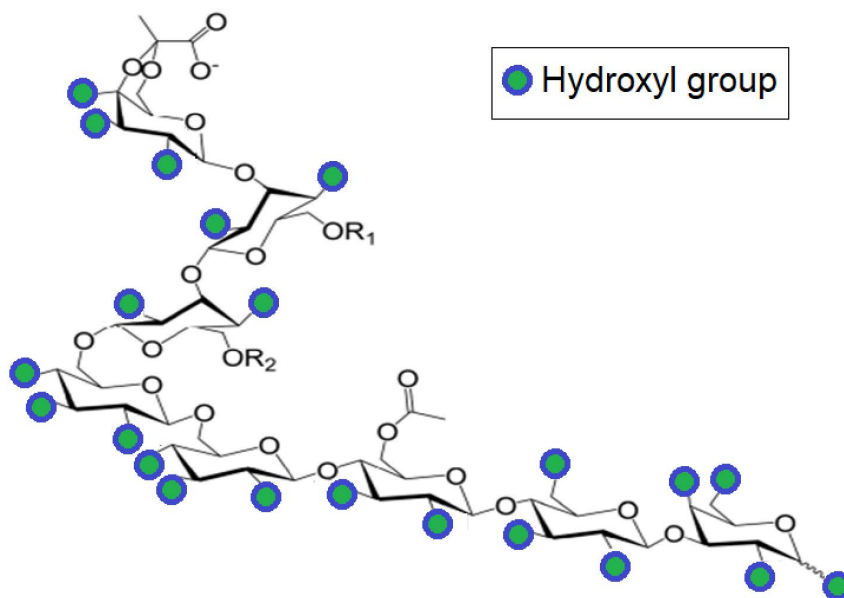
A totally different and more viable approach resides in reversibly capturing higher amounts of CO₂ than stoichiometry via weak carbonate-like associations with amphoteric to weakly basic hydroxyls of OH-functionalized materials [8,18–20]. Thus, CO₂ can be retained at standard temperature and pressure (STP) in CO₂-rich atmospheres and readily released upon forced convection under strong carrier gas stream or in CO₂-free media without heating, like in respiratory systems.

To meet these requirements, a judicious strategy involves the use of natural clay minerals such as Na⁺-exchanged montmorillonite (NaMt) that acts as an inorganic support in the preparation of CO₂ adsorbing materials [20]. Alkaline and alkaline

earth cations are known to display lower polarizing power and subsequently generate no Bronsted acidity via water molecule dissociation on clay surfaces dispersed in aqueous media. Alkaline-exchanged zeolites and clay minerals can even exhibit slight basicity that shades the slight acidity of the out-of-plane silanols [14,21]. Besides, lattice oxygen atoms surrounding the cation-exchangeable sites also act as Lewis basic sites making NaMt to show sufficient intrinsic surface basicity for retaining acidic gas such CO₂ [8,22]. An interesting alternative to improve the CO₂ retention capacity (CRC) of clay adsorbent would consist in the chemical grafting of an organic moiety bearing with large amount of hydroxyl sites [19]. The resulting organo-montmorillonite is expected to display additional amphoteric to slightly basic character and a more expanded structure with increased interfoliar spacing and porosity that favor CO₂ diffusion and storage.

In this work, rhizobial exopolysaccharide (EPS) (Scheme 1) was used as organic moiety to be grafted onto montmorillonite lamellar surface not only because of its sufficiently high amount of hydroxyl groups but also because of its natural sources. Indeed, EPS is a heteropolymer secreted by *Rhizobium* bacteria, and its structure comprises linear octa-saccharide subunits containing one galactose and seven glucose residues substituted with acetyl, pyruvil and succinyl groups [23–25]. The large amount of hydroxyl groups in EPS is expected to provide high number of adsorption sites capable of capturing CO₂ molecules through carbonate-like associations not only between next-neighboring CO₂ molecules but also with unavoidably adsorbed water molecules.

Such interactions are assumed to promote the retention of higher amounts of CO₂ than 1:1 stoichiometry via gas condensation around and between EPS moieties. Deeper insights through thermal programmed desorption (TPD) should provide valuable data on the adsorptive properties of the synthesized organo-montmorillonite in terms of both retention capacity and strength. Additional characterization by X-ray diffraction (XRD), infrared spectroscopy (FT-



Scheme 1. Molecular structure of an EPS monomer. R_1 and R_2 may also be hydrogen atoms depending on the hydroxylation grade.

IR) and thermogravimetry (TGA) would be useful for correlating the adsorption properties with the organoclay structure.

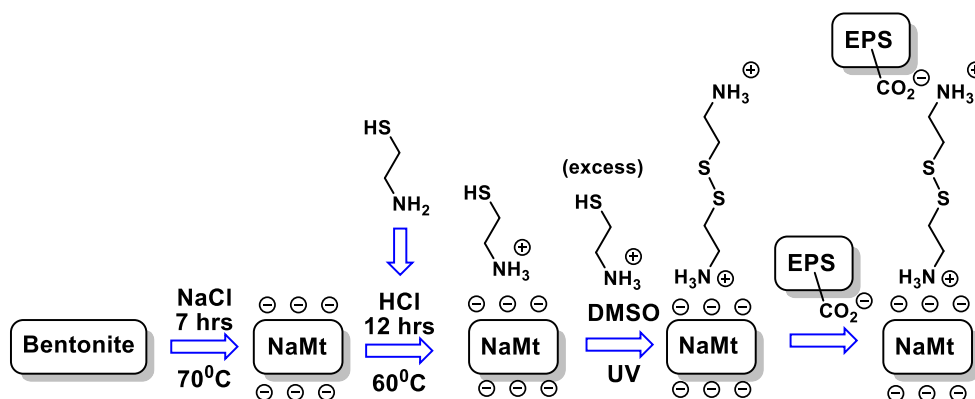
2. Experimental

2.1. Organo-montmorillonite preparation

Given that alkaline cations generate no Bronsted acidity on clay surfaces dispersed in aqueous media but rather exhibit slight basicity that shades the slight acidity of silanols, NaMt was prepared by bentonite purification in a NaCl aqueous solution. For this purpose, 100 g of bentonite (Aldrich) having a silica-to-alumina weight ratio of 2.98 was repeatedly impregnated by 1 L aqueous solution containing 233 g NaCl under continuous stirring at 70 °C for 7 hours. After settling, a 0.5 mm thin layer of the surface presumably containing organic impurities and the black-grey layer (1.0–1.5 cm) of the bottom supposed to mainly consist of volcanic ashes and denser phases were removed. The remaining intermediate layer was repeatedly washed with distilled water and centrifuged and then air dried overnight at 30–40 °C. Such a procedure of bentonite purification resulted in a clay material with a montmorillonite content

higher than 92%, due to the removal of dense silica phases such as quartz and cristobalite and other volcanic ashes.

2 g of the resulting dry NaMt was dispersed in distilled water and 0.8 g 2-mercaptoethylamine hydrochloride (Alfa Aesar) was added under vigorous stirring (Scheme 2). The mixture was heated at 60 °C for 12 hours, then centrifuged and repeatedly washed with distilled water and filtered, and finally dried in a rotary evaporator. Rhizobial EPS was previously extracted with a molecular weight cut-off (MWCO) higher than 10,000 Da against distilled water and then lyophilized, as defined for 90% of the macromolecules rejected by the separation membrane [23,26]. Thus, 200 mg of EPS was diluted in DMSO and stirred for 6 hours under UV radiations, and 400 mg of NaMt previously modified with 2-mercaptoethylamine hydrochloride was added to this mixture and stirred for 5 hours. The chemical grafting is expected to involve the formation of sulfur bridges between the previously anchored HS-Ethyl- NH_3^+ and dispersed EPS molecules upon UV radiation exposure. Two centrifugations of the resulting NaMt-EPS organoclay were performed, followed by drying using a rotary evaporator and then in a vacuum oven at 400 °C for 24 hours.



Scheme 2. EPS grafting on NaMt.

2-mercaptoethylamine hydrochloride is converted into 2-mercaptoethylammonium cation in acidic media, which is further grafted on NaMt surface through mere cation exchange into 2-mercaptoethyl- NH_3^+ -Mt-form. An excess of 2-mercaptoethyl- NH_3^+ should favor the oxidation of $-\text{SH}$ pairs generating a disulfide moiety ($-\text{S}-\text{S}-$) with two ammonium ends. The latter should act as an interface by simultaneously attracting negatively charged clay surface and carboxylate groups of EPS.

2.2. Characterization

The basal (001) spacing is a precise indicator of the interlayer spacing enlargement as a result of EPS incorporation. This feature was determined by XRD using a Siemens D5000 instrument ($\text{Co-}\alpha$ radiation at 1.7890 \AA). FT-IR spectra were recorded in the range $400\text{--}4000 \text{ cm}^{-1}$ by means of an IR550 Magna Nicolet equipment. The thermal stability was assessed in terms of decomposition threshold temperature of EPS through thermal gravimetric analysis on a TG/TDA6200 Seiko Instrument under a $120 \text{ mL}\cdot\text{min}^{-1}$ nitrogen stream and $5 \text{ }^\circ\text{C}\cdot\text{min}^{-1}$ heating rate.

2.3. Adsorptive feature assessment through TPD

The surface basicity and hydrophilic character were the main adsorptive features investigated herein in terms of CRC and water retention capacity (WRC). The CRC was evaluated through the total amount of desorbed CO_2 per gram of adsorbent powder after

full saturation at room temperature. The WRC accounts for the total amount of moisture contained in the starting non-dehydrated NaMt and in the saturating CO_2 used as the acidic probe gas. Both factors were measured by TPD according to a specific procedure [27]. This was achieved using a Li-840A dual $\text{CO}_2/\text{H}_2\text{O}$ Gas Analyzer. For this purpose, the powdered sample (40 mg) of $0.1\text{--}0.3 \text{ mm}$ particle size was introduced in a tubular reactor with 10 mm internal diameter, then dehydrated upon heating at $140 \text{ }^\circ\text{C}$ for 40 minutes under a $15 \text{ mL}\cdot\text{min}^{-1}$ dry nitrogen stream. In TPD measurements, the CO_2 and water retention strengths (CRS and WRS, respectively) are proportional to their corresponding desorption temperatures.

After cooling down to ambient temperature, the dry powder sample was kept in contact, till saturation, with oxygen-free dry CO_2 . The excess of non-adsorbed CO_2 was continuously evacuated at ambient temperature under $5 \text{ mL}\cdot\text{min}^{-1}$ dry nitrogen stream until a constant base line was obtained from the CO_2 detected at the reactor outlet. This optimal gas throughput was preliminarily found to allow full saturation with adsorption-desorption equilibrium without forced convection at ambient conditions [8,18–20,28]. These conditions allowed assessing accurately the CRC. The latter was calculated as the area of the TPD profile recorded between 20 and $190 \text{ }^\circ\text{C}$ at a constant $5 \text{ }^\circ\text{C}\cdot\text{min}^{-1}$ heating rate. This upper limit of the temperature range investigated herein was imposed by the decomposition threshold temperature of EPS as established by previous TGA measurements.

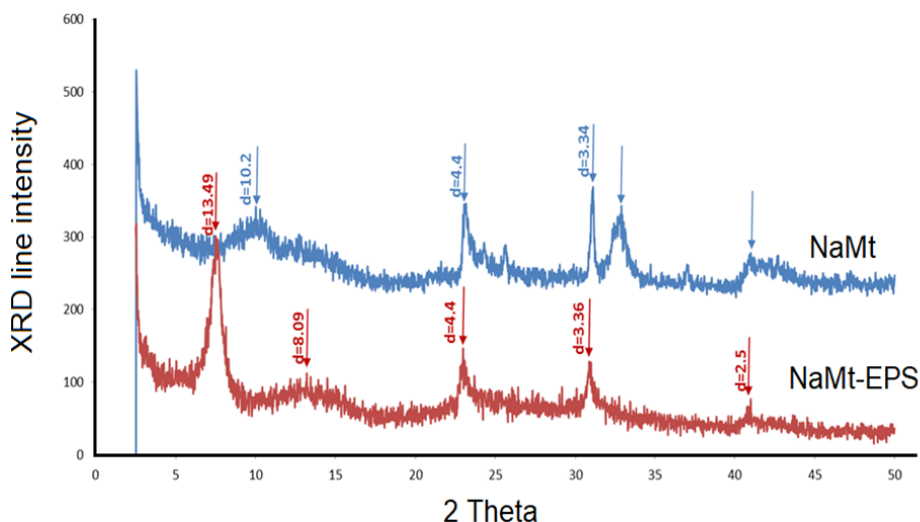


Figure 1. XRD patterns of NaMt and NaMt-EPS.

3. Results and discussion

3.1. Structural change upon EPS grafting

Comparison of the XRD spectra (Figure 1) revealed a marked sharpening of the line assigned to the (001) plane family and visible shift towards lower 2θ values upon EPS grafting. This accounts for an increase of the (001) basal spacing from 10.2 Å to 13.49 Å, i.e. an enlargement of the interlayer space of 3.29 Å. The latter is however smaller than the size of EPS molecules, and suggests a tilted layout of the grafted species. Such a layout can be explained by enhanced EPS–NaMt interaction at the expense of those occurring between EPS molecules and by the formation of higher number of H-bridges with the clay mineral surface. Such a structure expansion is expected to be beneficial for the adsorptive properties of the synthesized organoclay. Structure expansion offers increased accessible surface for adsorption, while high porosity allows easy diffusion towards the adsorption sites.

The (001) XRD line sharpening also indicates a transition from a random to a face-to-face parallel layout of the clay sheets [8,20,28–30]. This clearly demonstrates the uniform dispersion of the organic moiety within the interlayer space without EPS molecule aggregation into differently sized organic clusters. The latter are known to alter the face-to-face parallel layout of the clay lamellae as already re-

ported for other OH-enriched-montmorillonites [19, 20,28–33].

The marked depletion of the XRD line at 2θ of ca. 31, 32–33 and 41–43 degrees must be due to silanol and aluminol interactions with the hydroxyl groups of EPS. The preservation of the main XRD reflections of the preponderant smectite phase after EPS incorporation indicates that no structure alteration took place.

3.2. EPS interactions with NaMt

The incorporation of EPS on the clay mineral surface was supported by the appearance of new infrared bands at 2980 cm^{-1} and 2882 cm^{-1} attributed to both the asymmetric and symmetric stretching of the –CH bond (Figure 2). Special interest was devoted to a close-up focused in the IR bands observed in the broad region $3400\text{--}3700\text{ cm}^{-1}$. These bands are related to the most important factor for the adsorptive properties. The newly incorporated hydroxyl groups on the clay surface are expected to interact with silanols and siloxy group (Si–O–Si) thereby affecting the intrinsic moisture content of NaMt. The barely detectable absorption band around $3430\text{--}3450\text{ cm}^{-1}$ in NaMt accounts for overlapped antisymmetric and symmetric stretching vibrations of H-bridged water, while that around 3260 cm^{-1} is assigned to a bending mode of adsorbed water molecules.

These bands totally disappeared upon the rise of H-bridges with the incorporated hydroxyls of EPS

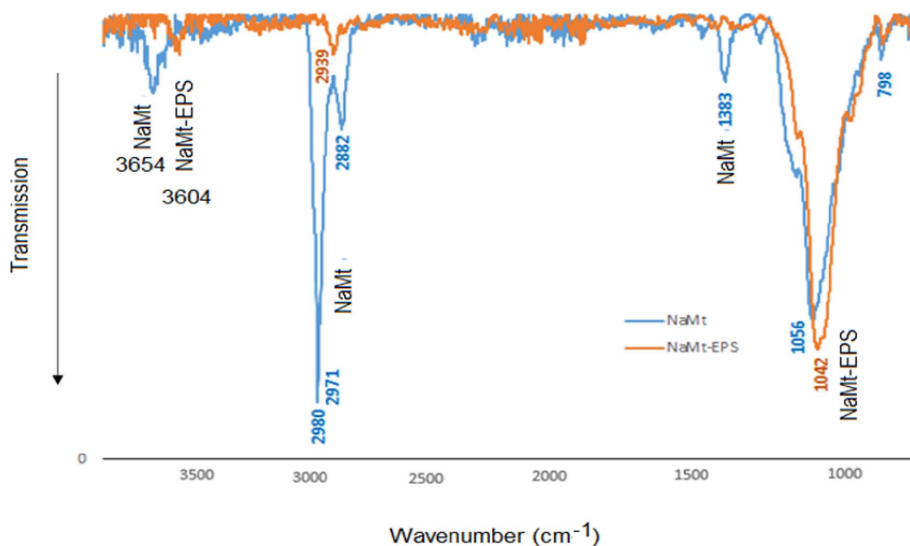


Figure 2. FT-IR spectra of NaMt (1) and NaMt-EPS (2).

at the expense of water molecules. The intensity increase in the stretching vibration band of the free OH groups around 3604 cm^{-1} provides clear evidence of the incorporation of increasing number of OH groups in the clay structure [34]. The shift of this band towards 3654 cm^{-1} indicates that at least a part of the OH groups of EPS are involved in interactions with the inorganic support and water molecules [35]. The bands observed at 1220 and 1042 cm^{-1} were attributed to the asymmetric stretching of the siloxy group. The slight intensity decrease of these bands and the slight shift of the 1042 cm^{-1} band to 1056 cm^{-1} must be due to the appearance of siloxy group interaction with the hydroxyls of EPS [36]. Clay silanols also appear to interact with EPS as supported by the intensity decay and noticeable shift of the 1604 cm^{-1} band up to 1632 cm^{-1} [30,37]. These results clearly demonstrate that the previous incorporation of the bi-ammonium cation as an interface between the clay mineral and EPS cannot prevent EPS–NaMt interactions.

3.3. Thermal stability

TGA analyzes of NaMt showed a barely detectable 1–2% weight loss due to dehydration, followed by an almost flat thermal profile, which indicates a total absence of additional thermal processes (Figure 3). EPS incorporation induced pronounced changes in

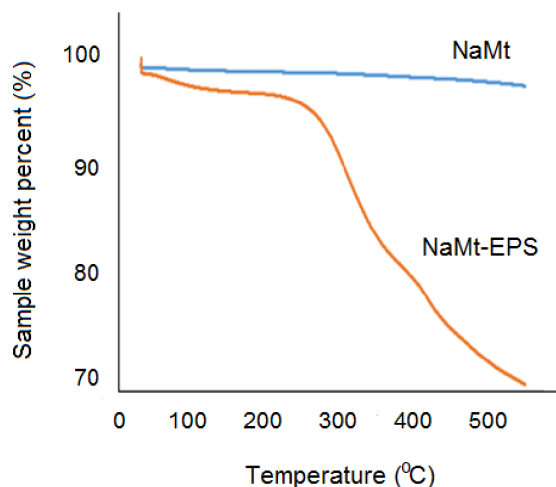


Figure 3. TGA patterns of NaMt and NaMt-EPS.

the TGA pattern. The appearance of a slightly higher moisture loss at $80\text{--}130^\circ\text{C}$ indicates an improvement of the hydrophilic character, presumably due to the incorporation of new hydroxyl groups. This weak dehydration of barely 3–4% contrasts with the relatively high number of OH groups brought by the 50 wt% EPS content loaded on NaMt. The most plausible explanation resides in the unavoidable formation of H-bridges between EPS molecules and with the clay mineral surface, as previously stated.

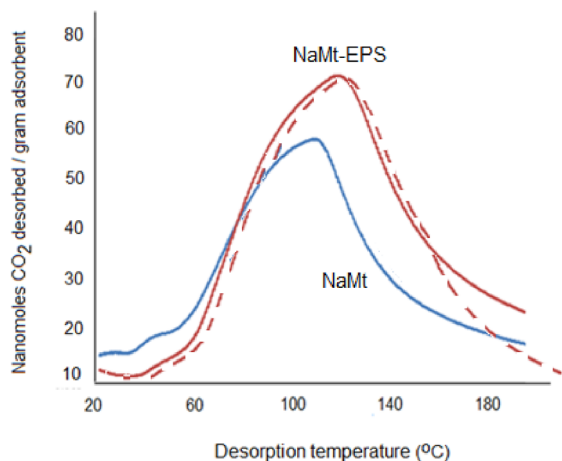


Figure 4. CO₂-TPD profiles of NaMt and NaMt-EPS. The dashed curve is a repeated CO₂-TPD profile of NaMt-EPS after the first profile and rehydration during re-saturation with a CO₂–water vapor mixture.

A second mass loss (15–16%) was triggered at 210–215 °C, most likely due to the thermal decomposition of the organic moiety. This accounts for the thermal stability threshold of the grafted EPS, which imposed the establishment of the upper limit for the TPD temperature range at 190 °C for an accurate assessment of the CRC. Since NaMt showed no other thermal process, the third weight loss (9–10%) noticed at ca. 350 °C must be due to a second decomposition step of EPS.

3.4. Affinity improvement towards CO₂

TPD profiles revealed almost symmetric shape of a single desorption peak for both NaMt and EPS-modified counterpart. This is precise indicator of the occurrence of CO₂ adsorption–desorption equilibrium that allows accurate CRC assessment within the investigated temperature range without gas loss by forced convection [8,18–20,28]. As expected, a significant increase in the amount of desorbed CO₂ was observed with increasing temperature for NaMt-EPS as compared to the starting NaMt material (Figure 4).

This accounts for an improvement of the affinity towards CO₂ for NaMt-EPS expressed in terms of higher CRC of ca. 820 $\mu\text{mol}\cdot\text{g}^{-1}$ as compared to NaMt

(670 $\mu\text{mol}\cdot\text{g}^{-1}$). This clearly demonstrates the beneficial effect of EPS grafting and contribution of newly introduced hydroxyl sites. These CRC values were assessed on the basis of the area described by the TPD profile in the range 20–190 °C, and are almost equal to the calculated values of the previously captured CO₂ during saturation at room temperature. According to the bell-shaped TPD diagrams on almost the same baseline, CO₂ appears to be completely desorbed upon slight heating up to 190 °C under this 15 mL·min^{−1} nitrogen stream, providing clear evidence of a truly reversible capture of CO₂.

The captured CO₂ appears to be weakly bound to the OH groups of EPS, most likely through the formation of hydrogen bridges and carbonate-like interactions between CO₂ and OH groups [18,36]. Such weak interactions were already found to allow total CO₂ release at ambient conditions via forced convection upon stronger carrier gas stream [8,18–20,28]. The 20 $\mu\text{mol}\cdot\text{g}^{-1}$ CRC is lower than the values reported for supported amines [38–40], mainly due to the compacted structure of NaMt-EPS as a result of hydroxyl interaction with the clay surface and next-neighboring EPS molecules. With specific surface not exceeding 40 m²·g^{−1}, which remains to be confirmed, NaMt-EPS is expected to display a surface affinity for CO₂ (SAC) of ca. 20–21 $\mu\text{mol}\cdot\text{m}^{-2}$ as defined by the CRC/Surface area ratio [17]. Compared to various highly porous materials [9–16,41] this value is lower than that of activated carbons (ca. 174 $\mu\text{mol}\cdot\text{m}^{-2}$) with CRC values of 103–217 mg CO₂·g^{−1} for specific surface area of 473–1361 m²·g^{−1} [11], but higher than that of modified polyacrylonitrile-based activated carbon fibers (ca. 1.75 $\mu\text{mol}\cdot\text{m}^{-2}$) with 2.74 mmol·g^{−1} CRC for a specific surface area of 1565 m²·g^{−1} [12].

The shift of the maximum of the sole desorption peak from ca. 110 °C (for NaMt) to approximately 125 °C (for NaMt-EPS) suggests a higher retention strength of CO₂ and a higher affinity of the organoclay, most likely due to additional interaction with retained moisture. This was supported by perfectly symmetrical TPD patterns obtained upon repetitive TPD cycles with alternate rehydration steps and by the absence of peak maximum shift with respect to NaMt without rehydration after each TPD cycles (Figures 4–5).

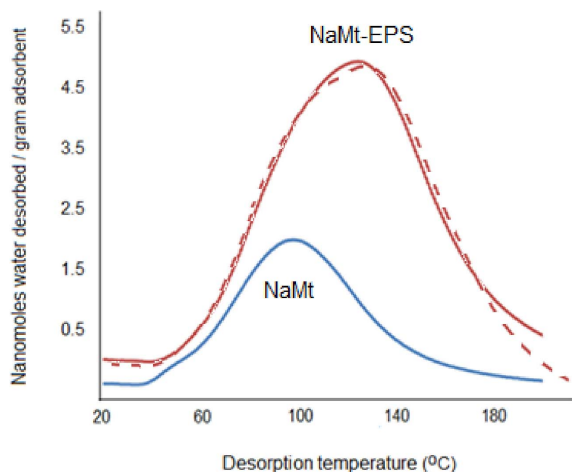


Figure 5. Water-TPD profiles of NaMt and NaMt-EPS. The dashed curve is a repeated Water-TPD profile of NaMt-EPS after the first profile and rehydration during re-saturation with a CO₂–water vapor mixture.

3.5. Hydrophilic character improvement

NaMt modification with EPS induced a marked improvement of the hydrophilic character herein expressed in terms of higher amounts of desorbed water within the same temperature range (Figure 5). In the meantime, a shift of the maximum of the water desorption peak from ca. 98–100 °C up to 125–128 °C. This indicates an enhancement of moisture retention strength, presumably by the same hydroxyl groups of EPS that also act as CO₂ adsorption sites. The fact that moisture retention involves H-bridges with the incorporated OH groups, it results that CO₂ adsorbs on moisture-containing EPS and clay surface via HO:CO₂ interactions as with alcohols [20,29,36, 42–45]. In other words, these simultaneous enhancements of both the surface basicity and hydrophilic character suggests the occurrence of a synergy that may also involve a ternary –HO:H–O–H:O=C=O interaction as reported earlier [29].

Here also, this accounts for an enhancement of WRS. This is most likely due to stronger interaction with adsorbed CO₂, inasmuch as no shift was observed in the absence of CO₂. This result is of great importance because it provides clear evidence of the occurrence of ternary –HO:H–O–H:O=C=O interaction. The latter should involve synergistic contribu-

tions of water and CO₂ in their retention in agreement with previous works [19].

The moisture content of NaMt-EPS showed a certain contribution to CO₂ retention in agreement with previous works [8,29]. The incorporated amount of EPS turned out to be suitable for inducing optimum surface properties, i.e. appreciable CRC by increased number of available OH groups involved in optimum interactions with both NaMt and surrounding CO₂ and water molecules. Such interactions prevent detrimental intermolecular aggregation of EPS into dense hydrophobic clusters [20,28,29].

4. Conclusion

Exopolyssacharide grafting on montmorillonite resulted in improved hydrophilic character and affinity towards CO₂ and of the hydrophilic character. The use of a disulfide ethyl moiety with two ammonium ends as interface produces a slight expansion of structure that facilitates the diffusion of CO₂ and water molecules, but cannot prevent H-bridges between EPS and the clay surface involving silanols and siloxy groups of NaMt. More than 16 CO₂ molecules appear to adsorb on one OH group incorporated, making NaMt-EPS to show a much higher surface affinity towards CO₂ as compared to most high surface-to-bulk adsorbents investigated so far. HO:CO₂ interactions between CO₂ molecules and both EPS and adsorbed water molecules appear to be responsible for synergetic CO₂ adsorption. CO₂ captured by OH-enriched organoclays was found to completely desorb at temperatures below 190 °C, without affecting the thermal stability of the adsorbent. These findings allow envisaging the design of OH-enriched organo-clays using plant-derived organic moieties for a truly reversible capture and concentration of non-stoichiometric amounts of CO₂ and consecutive regeneration with no or low energy consumption.

Conflicts of interest

Authors have no conflict of interest to declare.

Acknowledgments

This work was supported by grants from MDEIE-FQRNT (2011-GZ-138312) and FODAR-UQ-2015

(QC, Canada) to AA and RR. The authors are also grateful to Ana-Paula Beltrao-Nunes for her technical assistance.

References

- [1] R. Monastersky, *Nature*, 2009, **458**, 1091-1094.
- [2] A. Yamasaki, *J. Chem. Eng. Jpn.*, 2003, **36**, 361-375.
- [3] S. Cavenati, C. A. Grande, A. E. Rodrigues, *Chem. Eng. Sci.*, 2006, **61**, 3893-3906.
- [4] C. A. Grande, A. E. Rodrigues, *Int. J. Greenhouse Gas Control*, 2008, **2**, 194-202.
- [5] J. Zhang, P. A. Webley, P. Xiao, *Energy Convers. Manage.*, 2008, **49**, 346-356.
- [6] J. C. Abanades, E. S. Rubin, E. J. Anthony, *Ind. Eng. Chem. Res.*, 2004, **43**, 3462-3466.
- [7] S. Choi, J. H. Drese, C. W. Jones, *ChemSusChem*, 2009, **2**, 796-854.
- [8] A. Azzouz *et al.*, *Int. J. Greenhouse Gas Control*, 2013, **17**, 140-147.
- [9] J. Vieillard *et al.*, *J. Taiwan Inst. Chem. Eng.*, 2019, **95**, 452-465.
- [10] L. Giraldo, D. P. Vargas, J. C. Moreno-Piraján, *Front. Chem.*, 2020, **8**, article no. 543452.
- [11] S. Acevedo, L. Giraldo, J. C. Moreno-Piraján, *ACS Omega*, 2020, **5**, 10423-10432.
- [12] Y.-C. Chiang, C.-Y. Yeh, C.-H. Weng, *Appl. Sci.*, 2019, **9**, article no. 1977.
- [13] Y. Soujanya, *Adv. Carbon Capture*, 2020, **10**, 229-240.
- [14] C. Megías-Sayago *et al.*, *Front. Chem.*, 2019, **7**, 1-10.
- [15] R. Kusumastuti *et al.*, *J. Phys.: Conf. Ser.*, 2019, **1198**, article no. 032009.
- [16] M. Sai Bhargava Reddy *et al.*, *RSC Adv.*, 2021, **11**, 12658-12681.
- [17] A. Azzouz *et al.*, *Chem. Sus. Chem.*, 2015, **8**, 800-803.
- [18] A. Azzouz *et al.*, *Thermochim. Acta*, 2009, **496**, 45-49.
- [19] A. Azzouz *et al.*, *Mater. Res. Bull.*, 2013, **48**, 3466-3473.
- [20] A. Azzouz *et al.*, *Appl. Clay Sci.*, 2010, **48**, 133-137.
- [21] M. Sulpizi, M.-P. Gaigeot, M. Sprik, *J. Chem. Theory Comput.*, 2012, **8**, 1037-1047.
- [22] A. Azzouz *et al.*, *Adsorption*, 2013, **19**, 909-918.
- [23] E. Cho *et al.*, *Bull. Korean Chem. Soc.*, 2014, **35**, 2589-2592.
- [24] A. Skorupska *et al.*, *Microb. Cell Factories*, 2006, **5**, 1-19.
- [25] S. Kido *et al.*, *Biomacromolecules*, 2001, **2**, 952-957.
- [26] R. Singh, *Hybrid Membrane Systems for Water Purification: Technology, Systems Design and Operations*, Elsevier, Colorado Springs, USA, 2006.
- [27] A. Azzouz *et al.*, *Thermochim. Acta*, 2006, **449**, 27-34.
- [28] A. Azzouz *et al.*, *Sep. Purif. Technol.*, 2013, **108**, 181-188.
- [29] S. Nousir *et al.*, *J. Colloid Interface Sci.*, 2013, **402**, 215-222.
- [30] N. Bouazizi *et al.*, *J. Energy Inst.*, 2018, **91**, 110-119.
- [31] A. V. Arus *et al.*, *ChemistrySelect*, 2016, **1**, 1452-1461.
- [32] A. Azzouz *et al.*, *ChemSusChem*, 2015, **8**, 800-803.
- [33] A. Azzouz *et al.*, "Metal-organoclays as potentials adsorbents for hydrogen storage", in *2014 NSTI Nanotechnology Conference and Expo*, NSTI-Nanotech, Washington, National Harbor, 2014.
- [34] R. Sennour *et al.*, *Phys. Chem. Chem. Phys.*, 2017, **19**, 29333-29343.
- [35] S. Nousir *et al.*, *Can. J. Chem.*, 2017, **95**, 999-1007.
- [36] L. Aylmore, *Clays Clay Miner.*, 1974, **22**, 175-183.
- [37] N. Bouazizi *et al.*, *Appl. Surf. Sci.*, 2017, **402**, 314-322.
- [38] R. Serna-Guerrero, E. Da'na, A. Sayari, *Ind. Eng. Chem. Res.*, 2008, **47**, 9406-9412.
- [39] A. Sayari, Y. Belmabkhout, *J. Am. Chem. Soc.*, 2010, **132**, 6312-6314.
- [40] M. J. Lashaki, S. Khiavi, A. Sayari, *Chem. Soc. Rev.*, 2019, **48**, 3320-3405.
- [41] M. Pardakhti *et al.*, *ACS Appl. Mater. Interf.*, 2019, **11**, 34533-34559.
- [42] S. Gupta, R. Lesslie, A. King Jr, *J. Phys. Chem.*, 1973, **77**, 2011-2015.
- [43] R. Massoudi, A. King Jr, *J. Phys. Chem.*, 1973, **77**, 2016-2018.
- [44] M. Saharay, S. Balasubramanian, *J. Phys. Chem. B*, 2006, **110**, 3782-3790.
- [45] J. J. Gassensmith *et al.*, *J. Am. Chem. Soc.*, 2011, **133**, 15312-15315.